Materials Physics and Mechanics. 2023;51(5): 107-114
Research article
http://dx.doi.org/10.18149/MPM.5152023_11

Submitted: March 3, 2023
Approved: March 20, 2023
Accepted: April 10, 2023

Effect of Al addition on the mechanical properties of $Zr_{50}Cu_{50-x}Al_x$ (0≤x≤50) bulk metallic glass

V. Guder

Trakya University, Edirne, Turkey

✉ vildanguder@trakya.edu.tr

Abstract. The evolution of microstructural and mechanical properties of ternary Zr-Cu-Al metallic glass under tensile loading was investigated by molecular dynamics simulations using embedded atomic potentials to describe interactions between atoms in the system. Special attention was paid to the variation of these properties according to the Al content in the $Zr_{50}Cu_{50-x}Al_x$ (0≤x≤50) system. The results showed that there is no systematic relationship between the elastic properties and the amount of Al, but the local structure of the system is significantly affected during the tensile load. The elastic modulus and yield stress were found to be maximum at 40 and 20 %, respectively. It was also revealed that the addition of Al decreased the fraction of Al-centered <0,0,12,0> polyhedra, and increased the fraction of the same polyhedra around Cu and Zr.

Keywords: molecular dynamics simulations; elastic modulus; voronoi polyhedral; mechanical properties; ZrCuAl metallic glass

Citation: Guder V. Effect of Al addition on the mechanical properties of $Zr_{50}Cu_{50-x}Al_x$ (0≤x≤50) bulk metallic glass. Materials Physics and Mechanics. 2023;51(5): 107-114. DOI: 10.18149/MPM.5152023_11.

Introduction

Zr-based bulk metallic glasses (BMGs), which are among the BMG that have attracted great attention due to their physical, mechanical and chemical properties, have attracted attention due to their high glass-forming ability (GFA) [1–3]. Properties such as ease of formability, low Elastic Modulus, high elastic strain and yield strength make BMGs very useful for structural applications. It is known that suppression of crystal nucleation and enhancement of GFA can be achieved by the addition of a third element [4,5]. The ternary Cu-Zr-Al systems have a large supercooled liquid region and high mechanical strength [6]. It has been observed that the addition of Al to the $Cu_{50}Zr_{50}$ system caused significant plastic deformation and increased the GFA [4–7]. $Zr_{30}Cu_{60}Al_{10}$ shows better GFA, higher stiffness and strength [8]. The ductility is observed as a result of nucleation of shear bands for $Cu_{47.5}Zr_{47.5}Al_5$ BMG, while brittleness is observed as a result of rapid propagation of shear bands by fracturing an amorphous phase for $Cu_{46}Zr_{47}Al_7$ BMG [7]. The improved GFA and high viscosity value due to the denser liquid structure of $(Cu_{50}Zr_{50})_{95}Al_5$ alloy compared with the $Cu_{50}Zr_{50}$ alloy is reported [9]. For $Zr_{50}Cu_{50-x}Al_x$ systems, it has been found that the alloys of x≤20 have the best GFA and Al is the active element in controlling GFA [10]. Al content cause amorphization and more pronounced amorphization has been observed for $Zr_{50}Cu_{44}Al_6$ and $Zr_{50}Cu_{40}Al_{10}$ alloys [11]. For $Cu_{50}Zr_{50-x}Al_x$ alloys, the range is 0≤x≤4 for non-eutectic alloys, while the range to eutectic composition is 5≤x≤11. $Cu_{50}Zr_{47}Al_3$ alloy has the best GFA, lowest brittleness index and highest fracture strength [12]. The glass transition temperature (T_g), the initial crystallization

© V. Guder, 2023.
Publisher: Peter the Great St. Petersburg Polytechnic University
This is an open access article under the CC BY-NC 4.0 license (https://creativecommons.org/li-censes/by-nc/4.0/)

temperature (T_x) and supercooled liquid region, hardness and Elastic Modulus increase with increasing Al concentration for $(Cu_{50}Zr_{50})_{100-x}Al_x$ (x=0–12). Cheung and Shek have reported that the hardness was smallest for $Cu_{50}Zr_{50}$ and greatest for $(Cu_{50}Zr_{50})_{90}Al_{10}$ [13]. The T_x, yield and fracture strength increase with increasing Al content for $(Cu_{50}Zr_{50})_{100-x}Al_x$ (x=0-6) metallic glass wires [14]. It has been found that T_g, fracture strength and hardness decreased, and Elastic Modulus, Debye temperature and shear modulus increased with the addition of Al for $Cu_{50}Zr_{50}$ [15]. The crystal nucleation in the system is suppressed with the addition of 7 % of Al to the $Cu_{50}Zr_{50}$ amorphous system [19]. It is seen that the studies on Zr-Cu-Al described above are mostly limited to the addition of Al content in small amounts. In this study, the influence of mechanical and structural properties in a wide range of Al amounts for $Zr_{50}Cu_{50-x}Al_x$ ($0 \leq x \leq 50$). The results are discussed in detail in terms of the local environment and atomic localization.

Method

A Large – scale Atomic-Molecular Massively Parallel Simulator (LAMMPS) served as an open-source code [16] was used to investigate effects of Al addition on the mechanical properties of $Zr_{50}Cu_{50-x}Al_x$ ($0 \leq x \leq 50$) bulk metallic glass during tensile process. The reliability of the MD simulation strongly depends on the interatomic potential, which can better explain the atomic interactions of the system. Embedded atom method (EAM) potential was used for the Zr–Cu–Al system, which was successful in simulating existing binary and ternary metallic glasses [17,18]. In order to construct a ternary $Zr_{50}Cu_{40}Al_{10}$ crystalline system, the simulation box was taken as body-centered cubic (BCC) with 31250 atoms and the lattice constant was taken as 3.283 Å. The snapshot of the initial model is given in Fig. 1(a). After the energy minimization, the system was heated from 50 to 2050 K with a heating rate of 0.5 K/ps using an isothermal-isobaric ensemble with a constant number of particles, pressure and temperature (NPT). The time step was 0.001 ps. The snapshot of the model system in the liquid state is given in Fig. 1(b). The liquid model obtained for $Zr_{50}Cu_{40}Al_{10}$ alloy was used to construct the initial configuration of $Zr_{50}Cu_{50}$, $Zr_{50}Cu_{45}Al_5$, $Zr_{50}Cu_{35}Al_{15}$, $Zr_{50}Cu_{30}Al_{20}$, $Zr_{50}Cu_{25}Al_{25}$, $Zr_{50}Cu_{20}Al_{30}$, $Zr_{50}Cu_{15}Al_{35}$, $Zr_{50}Cu_{10}Al_{40}$, $Zr_{50}Cu_5Al_{45}$ and $Zr_{50}Al_{50}$ liquid systems by changing the Al concentration. After adjusting the atom labels to guarantee the composition of alloys, these systems were subjected to a 100 ps equilibration at 2050 K and cooled to 300 K with a cooling rate of 0.1 K/ps applying the periodic boundary conditions through x-, y- and z-directions. Obtained amorphous systems for $Zr_{50}Cu_{40}Al_{10}$ and other compositions are shown in Fig. 1(c) and Fig. 2.

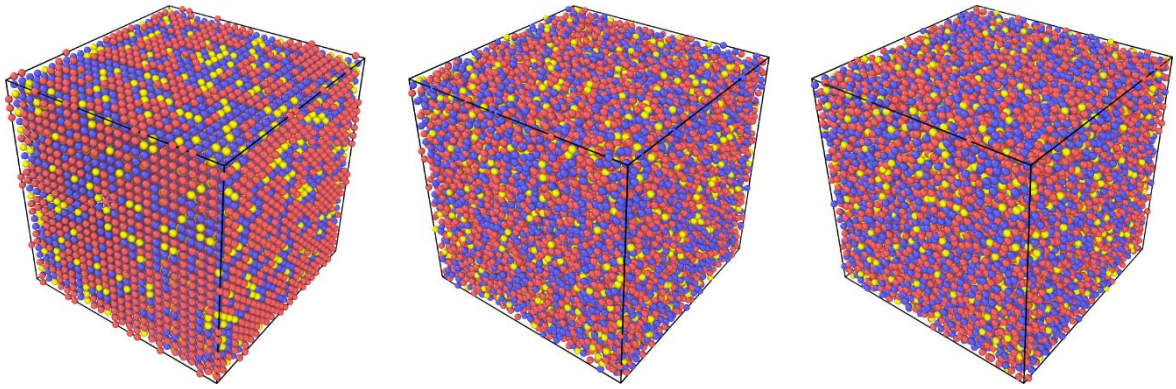

(a) (b) (c)

Fig. 1. MD simulation snapshots (a) initial crystalline (b) liquid (c) amorphous for $Zr_{50}Cu_{40}Al_{10}$ system. The red, blue and yellow spheres represent Zr, Cu and Al atoms, respectively

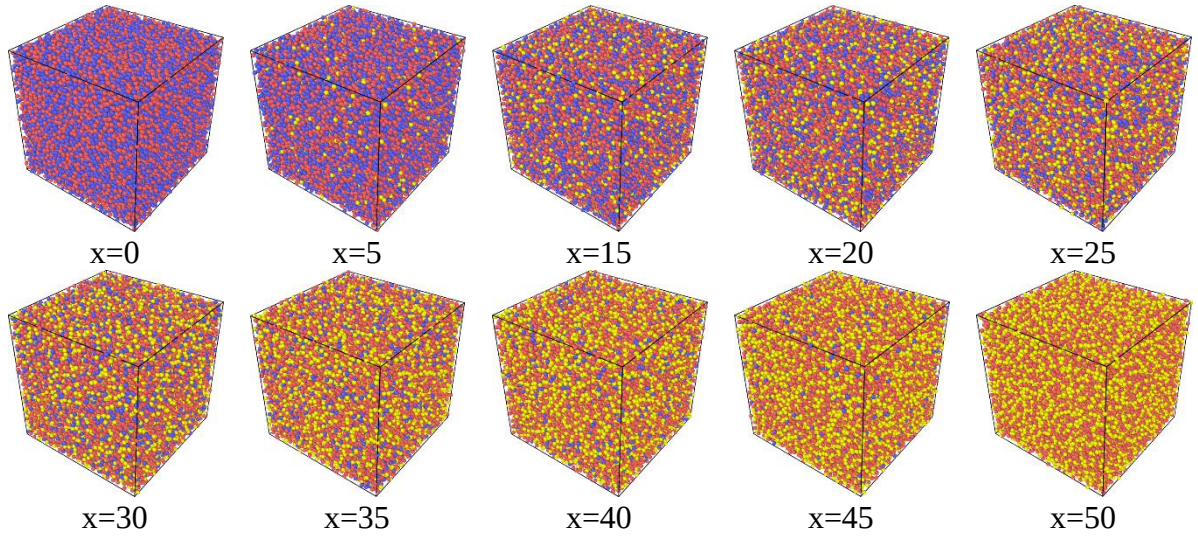

Fig. 2. MD simulation snapshots for amorphous $Zr_{50}Cu_{50-x}Al_x$ (0≤x≤50) systems. The red, blue and yellow spheres represent Zr, Cu and Al atoms, respectively

Before loading, each amorphous system has been relaxed with 100 ps under the microcanonical ensemble of NVE (N atomic number, V volume, E total energy) to obtain an equilibrium state at 300 K. For all amorphous systems, uniaxial stress was applied along the z-direction. During the tensile deformation, the periodic boundary conditions were applied along the three directions of Cartesian coordinates. In this method, while the periodic length in the z-direction increases with the applied strain rate, the other two directions (ie x- and y-) are allowed to change to keep the pressure in these directions equal to zero. The temperature was kept at 300 K based on the Nose-Hoover thermostat, each amorphous system was elongated by 10 % during the tensile deformation at the strain rate of 0.0001 ps^{-1} with the isothermal-isobaric (NPT) ensemble.

Results and Discussions

The stress-strain curves guide to investigate of the effects of Al addition on the mechanical properties of $Zr_{50}Cu_{50-x}Al_x$ (0≤x≤50) bulk metallic glass. Figure 3(a) shows that stress-strain curves for $Zr_{50}Cu_{50-x}Al_x$ bulk metallic glass during tensile deformation. The region in which the atoms maintain their regular lattice arrangement is called the elastic region. The stress and strain at the boundary of the elastic region correspond to the yield stress and yield strain, respectively. In this study, the stress corresponding to the strain value of 0.04 in which the linearity of the stress-strain curve deteriorates has called yield stress. For amorphous systems, stress-strain curves show smooth transition behaviour after the elastic region, indicating that the small deformation region is enlarged and spread throughout the system and the deformation is homogeneous. The highest value of the stress in the stress-strain curve during all tensile deformation is called the ultimate stress. The ultimate stress for $Zr_{50}Cu_{50}$ is 1.85 GPa which agrees with experimental data (1.88 GPa) [7]. Figure 3(b) shows that the variation of yield stress depending on Al amount for $Zr_{50}Cu_{50-x}Al_x$ (0≤x≤50) bulk metallic glass. The yield stress increases from x=0 to x=10 and decreases sharply at x=15. A maximum value at x = 20 is followed by zigzag behavior. In this case, $Zr_{50}Cu_{30}Al_{20}$ has the highest strength. The value of yield stress is almost the same for $Zr_{50}Cu_{50}$ and $Zr_{50}Al_{50}$, $Zr_{50}Cu_{45}Al_5$ and $Zr_{50}Cu_5Al_{45}$, $Zr_{50}Cu_{40}Al_{10}$ and $Zr_{50}Cu_{10}Al_{40}$. The yield stress for $Zr_{50}Cu_{40}Al_{10}$ is 1.91 GPa which is a fair agreement with experimental data (1.86 GPa) [19].

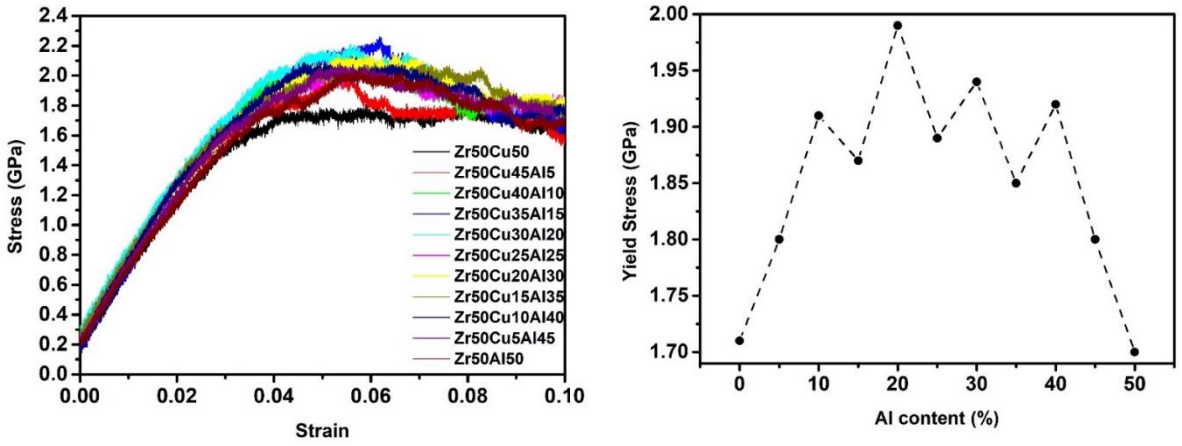

(a) (b)

Fig. 3. For $Zr_{50}Cu_{50-x}Al_x$ ($0 \leq x \leq 50$) bulk metallic glass (a) stress-strain curves (b) yield stress variation depending on Al concentration

Elastic modulus is known as a measure of elastic deformation under applied tensile loading and is calculated from the slope of stress-strain curves up to a strain value of 0.015 in present work. Figure 4 shows that elastic modulus variation depending on Al content for $Zr_{50}Cu_{50-x}Al_x$ ($0 \leq x \leq 50$) bulk metallic glass. There is no clear relationship between Al concentration and Elastic Modulus. In the range of Al amount studied in this study, the Elastic Modulus of $Zr_{50}Cu_{50}$ is minimum which reflects its flexible nature while the elastic modulus of $Zr_{50}Cu_{10}Al_{40}$ is maximum which is a sign of a stiffer material. Table 1 lists elastic modulus values for $Zr_{50}Cu_{50-x}Al_x$ (x=0,10). Elastic modulus values obtained in this study are compatible with the literature. However, the Elastic modulus obtained by molecular dynamics simulation is different from that obtained from the experimental study due to the small size of the metallic glasses used in MD simulation and ignoring the defects and cracks in the sample during simulations.

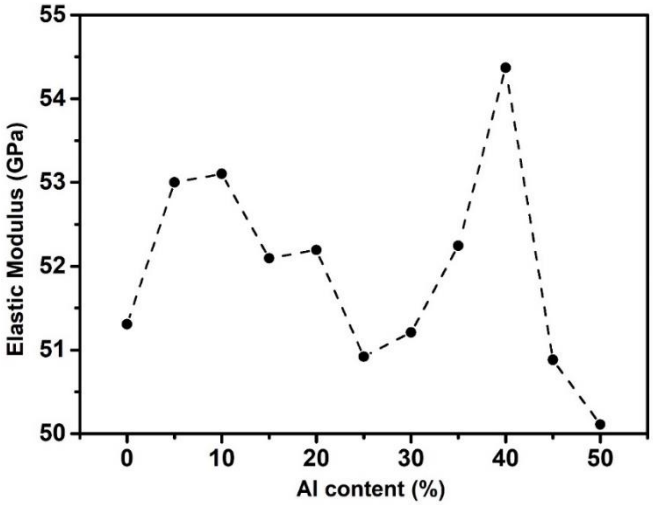

Fig. 4. Elastic modulus variation depending on Al concentration for $Zr_{50}Cu_{50-x}Al_x$ ($0 \leq x \leq 50$) bulk metallic glass

Table 1. Elastic Modulus values for $Zr_{50}Cu_{50-x}Al_x$ (x=0,10)

	This work, GPa	Exp., GPa	Other, GPa
$Zr_{50}Cu_{50}$	51.3	-	55[a]
$Zr_{50}Cu_{40}Al_{10}$	53.1	88[b]	59[c]

[a][20], [b][19], [c][8]

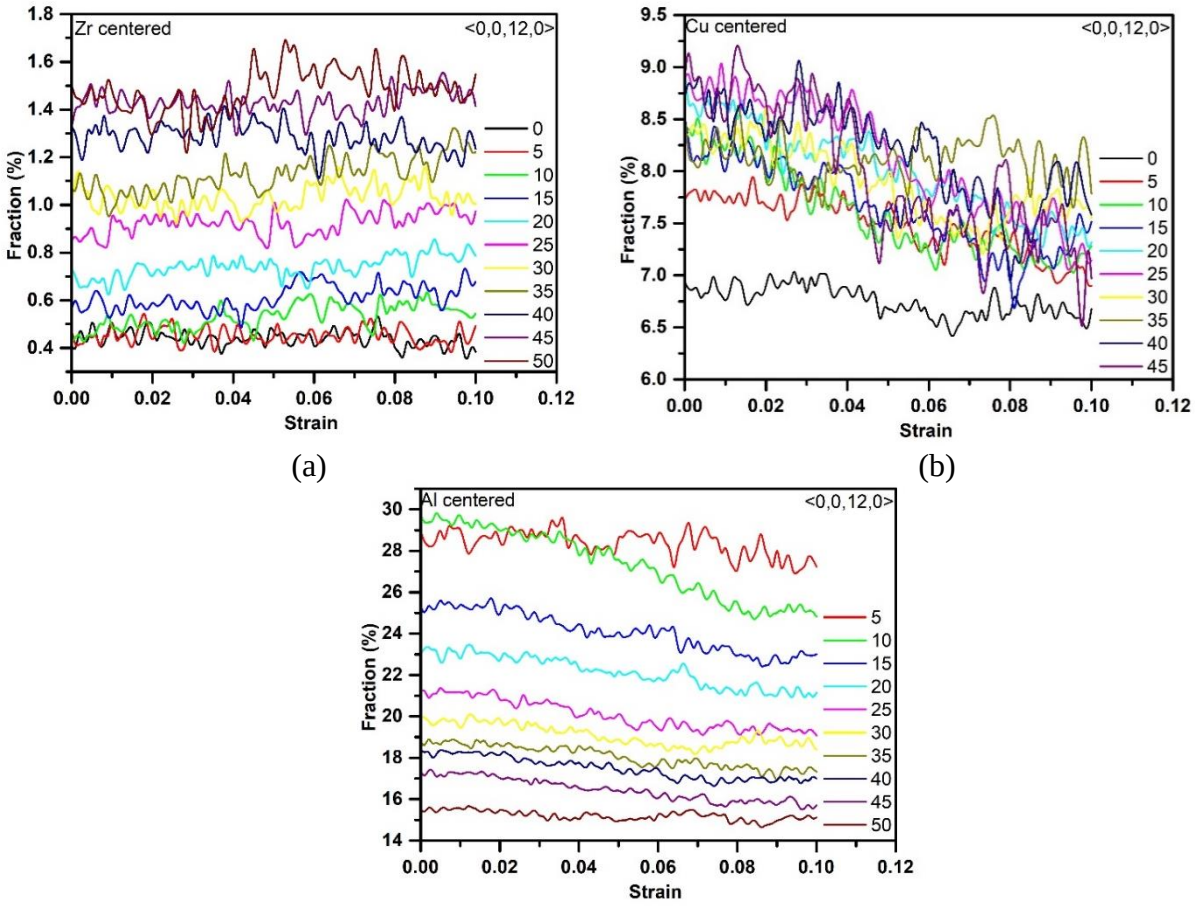

Fig. 5. The variation of (a) Zr (b) Cu (c) Al centered <0,0,0,12> VPs with strain for $Zr_{50}Cu_{50-x}Al_x$ (0≤x≤50) BMGs

The Voronoi tessellation method [21,22] gives us detailed information about the local atomic structure of the system and the variation of local clusters during the tensile process. In the Voronoi tessellation method, the polyhedra in the system are defined by connecting each atom with an index $<n_3,n_4,n_5,n_6>$ where n_i is the number of faces with i vertices of the VP. In this study, ideal icosahedral (ico) and icosahedra-like (ico-like) VPs were categorized according to reference [23,24]. Ideal ico is defined by <0,0,12,0> VP while ico-like are presented by <0,2,8,x>, <0,0,12,x> and <0,1,10,x> VPs (x=2-6). Figure 5 shows that the variation of (a) Zr (b) Cu (c) Al centered <0,0,0,12> VPs as a function of strain. Due to the Zr content being kept constant in the system, the <0,0,0,12> VPs fraction around Zr atoms is not affected by strain except for the slight deviation observed in the range between the yield and ultimate strains. While Cu and Al centered <0,0,0.12> VPs are almost unchanged up to the value of yield strain (value of 0.004), these tend to decrease with increasing strain. Before the tensile loading, it is observed that the addition of Al decreases the fraction of Al-centered <0,0,12,0> polyhedra, and increased the fraction of the same polyhedra around Cu and Zr. The fraction of Al centered <0,0,12,0> clusters is higher than that of other constituent atoms. For $Zr_{50}Cu_{40}Al_{10}$, its value is 29 % which is the maximum before loading. It decreases with strain. The material resists corrosion thanks to the presence of <0,0,12,0> clusters [25]. Al atoms can be considered as the key factor in resisting corrosion of the amorphous system.

Figure 6 shows that the variation of (a) Zr (b) Cu (c) Al centered ico-like VPs with strain for $Zr_{50}Cu_{50-x}Al_x$ (0≤x≤50). In Figure 5, the ico-like VPs at the relevant atomic centered are represented as follows. Zr centered ico-like is the sum of the fraction of <0,2,8,2>, <0,2,8,3>,

<0,2,8,4>, <0,2,8,5>, <0,2,8,6>, <0,1,10,2>, <0,1,10,3>, <0,1,10,4>, <0,1,10,5>, <0,0,12,0>, <0,0,12,2>, <0,0,12,3> and <0,0,12,4> VPs. Cu centered ico-like is the sum of the fraction of <0,2,8,0>, <0,2,8,1>, <0,2,8,2>, and <0,0,12,0> VPs. Al centered ico-like is the sum of the fraction of <0,2,8,0>, <0,2,8,1>, <0,2,8,2>, <0,2,8,3>, <0,1,10,2> and <0,0,12,0> VPs. Zr centered ico-like VPs are numerous and diverse. It is revealed that the addition of Al decreases the fraction of Al-centered ico-like polyhedra, and increases the fraction of the same polyhedra around Cu and Zr. With increasing strain, Zr and Cu centered ico-like VPs decrease, while Al centered same VPs tend to decrease vaguely.

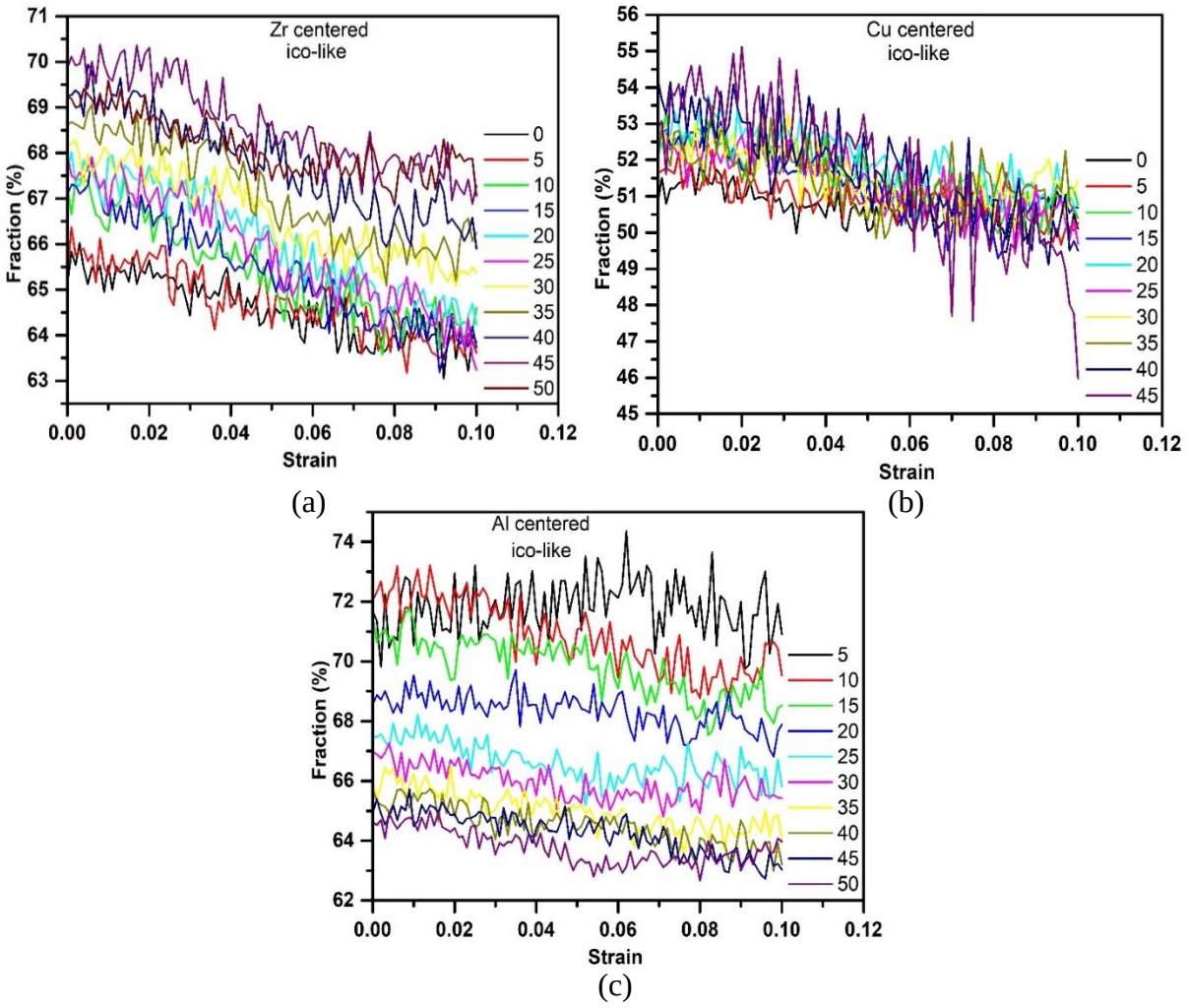

Fig. 6. The variation of (a) Zr (b) Cu (c) Al centered ico-like VPs with strain for $Zr_{50}Cu_{50-x}Al_x$ ($0 \leq x \leq 50$) BMGs

Conclusion

The evolution of microstructural and mechanical properties of ternary Zr-Cu-Al metallic glass under tensile loading was investigated by molecular dynamics simulations using embedded atomic potentials to describe interactions between atoms in the system. It is observed that $Zr_{50}Cu_{30}Al_{20}$ has the highest strength, while $Zr_{50}Al_{50}$ and $Zr_{50}Cu_{50}$ have the lowest. Additionally, $Zr_{50}Cu_{50}$ is a more flexible material than the other compositions, while $Zr_{50}Cu_{10}Al_{40}$ is a stiffer. The value of yield stress and Elastic Modulus for some $Zr_{50}Cu_{50-x}Al_x$ ($0 \leq x \leq 50$) alloys are in agreement with the literature. The fraction of ideal-ico clusters around the Al varies between 15 and 29 % and this ratio is higher than other related atoms. Due to the <0,0,0,12> VP constituting the most stable geometric units and forms to the essence of

icosahedral short range, we observed that for BMG, Al atoms dominate the local icosahedral short range. Additionally, Al atoms can be considered as the key factor in resisting corrosion of the amorphous system.

References

1. Zhang GQ, Jiang QK, Chen LY, Shao M, Liu JF, Jiang JZ. Synthesis of centimeter-size Ag-doped Zr–Cu–Al metallic glasses with large plasticity. *J. Alloys Compd*. 2006;424(1–2): 176–178.
2. Peker A, Johnson WL. A highly processable metallic glass: Zr 41.2 Ti 13.8 Cu 12.5 Ni 10.0 Be 22.5. *Appl. Phys. Lett.* 1993;63(17): 2342–2344.
3. Romanov AI, Panov VA, Samsonov MA, Chirkin DE, Bragov AM, Igumnov LA, et al. Study of the deformation and fracture of zirconium alloys under dynamic loading. *Mater. Phys. Mech.* 2020;46(1): 88–98.
4. Das J, Tang MB, Kim KB, Theissmann R, Baier F, Wang WH, et al. "Work-Hardenable" Ductile Bulk Metallic Glass. *Phys. Rev. Lett.* 2005;94(20): 205501.
5. Yu P, Bai HY, Tang MB, Wang WL. Excellent glass-forming ability in simple Cu50Zr50-based alloys. *J. Non Cryst. Solids.* 2005;351(14–15): 1328–1332.
6. Inoue A, Zhang W. Formation, Thermal Stability and Mechanical Properties of Cu-Zr-Al Bulk Glassy Alloys. *Mater. Trans.* 2002;43(11): 2921–2925.
7. Baser TA, Das J, Eckert J, Baricco M. Glass formation and mechanical properties of (Cu50Zr50)100−xAlx (x=0, 4, 5, 7) bulk metallic glasses. *J. Alloys Compd.* 2009;483(1–2): 146–149.
8. Deb Nath SK. Formation, microstructure and mechanical properties of ternary ZrxCu90−xAl10 metallic glasses. *J. Non Cryst. Solids.* 2015;409: 95–105.
9. Fan GJ, Freels M, Choo H, Liaw PK, Li JJZ, Rhim WK, et al. Thermophysical and elastic properties of Cu50Zr50 and (Cu50Zr50)95Al5 bulk-metallic-glass-forming alloys. *Appl. Phys. Lett.* 2006;89(24): 241917.
10. Celtek M, Sengul S, Domekeli U. Glass formation and structural properties of Zr50Cu50-xAlx bulk metallic glasses investigated by molecular dynamics simulations. *Intermetallics.* 2017;84: 62–73.
11. Meng FQ, Tsuchiya K, Yokoyama Y. Crystalline to amorphous transformation in Zr-Cu-Al alloys induced by high pressure torsion. *Intermetallics*. 2013;37: 52–58.
12. Cai A, Liu Y, Wu H, Ding D, An W, Zhou G, et al. Phase formation, glass forming ability, mechanical and thermal properties of Cu50Zr50−x Al x (0⩽x⩽11.0) glass forming alloys. *Sci. China Mater.* 2015;58(7): 584–594.
13. Cheung TL, Shek CH. Thermal and mechanical properties of Cu–Zr–Al bulk metallic glasses. *J. Alloys Compd.* 2007;434–435: 71–74.
14. Liao W, Zhao Y, He J, Zhang Y. Tensile deformation behaviors and damping properties of small-sized Cu–Zr–Al metallic glasses. *J. Alloys Compd.* 2013;555: 357–361.
15. Wang WH. The elastic properties, elastic models and elastic perspectives of metallic glasses. *Prog. Mater. Sci.* 2012;57(3): 487–656.
16. Plimpton S. Fast Parallel Algorithms for Short-Range Molecular Dynamics. *J. Comput. Phys.* 1995:117(1): 1–19.
17. Cheng YQ, Ma E, Sheng HW. Atomic Level Structure in Multicomponent Bulk Metallic Glass. *Phys. Rev. Lett.* 2009;102(24): 245501.
18. Sheng HW, Kramer MJ, Cadien A, Fujita T, Chen MW. Highly optimized embedded-atom-method potentials for fourteen fcc metals. *Phys. Rev. B.* 2011;83(13): 134118.
19. Yokoyama Y, Yamasaki T, Liaw PK, Inoue A. Study of the structural relaxation-induced embrittlement of hypoeutectic Zr–Cu–Al ternary bulk glassy alloys. *Acta Mater.* 2008;56(20): 6097–6108.
20. Feng SD, Li L, Chan KC, Qi L, Zhao L, Wang LM, et al. Control of shear band dynamics in Cu50Zr50 metallic glass by introducing amorphous-crystalline interfaces. *J. Alloys Compd.* 2019;770: 896–905.
21. Voronoi G. New Parametric Applications Concerning the Theory of Quadratic Forms -

Second Announcement. *J. Reine Angew Math.* 1908;134: 198–287.
22. Rycroft CH. VORO++ : A three-dimensional Voronoi cell library in C++. *Chaos: An Interdiscip J. Nonlinear Sci.* 2009;19(4): 041111.
23. Zhang P, Maldonis JJ, Besser MF, Kramer MJ, Voyles PM. Medium-range structure and glass forming ability in Zr–Cu–Al bulk metallic glasses. *Acta Mater.* 2016;109: 103–114.
24. Kbirou M, Trady S, Hasnaoui A, Mazroui M. Cooling rate dependence and local structure in aluminum monatomic metallic glass. *Philos. Mag.* 2017;97(30): 2753-2771.
25. Park KW, Fleury E, Seok HK, Kim YC. Deformation behaviors under tension and compression: Atomic simulation of Cu65Zr35 metallic glass. *Intermetallics.* 2011;19(8): 1168–1173.

THE AUTHOR

V. Guder
e-mail: vildanguder@trakya.edu.tr